OPTIMIZATION OF LOW-PRESSURE AXIAL FANS AND EFFECT OF SUBSEQUENT GEOMETRICAL MODIFICATIONS

Konrad BAMBERGER[1], Thomas CAROLUS[1],
Markus HAAS[2]

[1] *Institute for Fluid- and Thermodynamics, University of Siegen, Paul-Bonatz-Str. 9-11, 57068 Siegen, Germany*

[2] *Helios Ventilatoren GmbH & Co KG, Lupferstr.8, 78056 Villingen-Schwenningen*

SUMMARY

An evolutionary algorithm is used to optimize an axial fan with respect to total-to-static efficiency at a given design point. In the algorithm, the target function is evaluated by artificial neural networks (ANN). The optimized design is simulated by means of CFD and investigated experimentally. The two methods show good agreement. After that, the impact of subsequent geometrical changes is investigated. Firstly, the tip clearance is increased from 0.1% of the fan diameter to the more practical value of 0.5%. Secondly, the cylindrical hub is replaced by a narrow disc. Both changes reduce the peak efficiency by around seven percentage points and compromise the operating range.

NOMENCLATURE

Latin symbols

D	diameter
P	power
S	tip clearance
$\dot{V}$	flow rate
c	chord length
d	max. thickness of NACA airfoils
f	max. camber of NACA airfoils
l	length
n	fan speed
p	pressure
x	coordinate along the chord

Greek Symbols

α	weighting factor for penalty terms
δ	specific fan diameter
γ	stagger angle
ϕ	flow coefficient
η	efficiency
ν	hub-to-tip ratio
ρ	air density
σ	specific fan speed
ψ	pressure coefficient

Indices

1	upstream of the fan
2	downstream of the fan
ax	axial
t	total
ts	total-to-static

Abbreviations

ANN	artificial neural network
CFD	computational fluid dynamics
MLP	multi-layer perceptron
PT	penalty term
RANS	Reynolds-averaged Navier-Stokes

INTRODUCTION

An industrial fan which fulfils the characteristic curve in Figure 1 shall be developed. The curve is plotted dimensionless, i.e. the flow rate $\dot{V}$ and the pressure rise Δp are normalized with the fan diameter D, the fan speed n and the air density ρ yielding the flow coefficient ϕ and the pressure coefficient ψ, respectively:

$$\phi = \frac{\dot{V}}{\frac{\pi^2}{4} D^3 n} \tag{1}$$

$$\psi = \frac{\Delta p}{\frac{\pi^2}{2} D^2 n^2 \rho} \tag{2}$$

In the intended application of the fan, the kinetic energy at the fan exit is useless as it dissipates in the surroundings. Hence, we define Δp as the total-to-static pressure rise (index "*ts*") which is the static pressure downstream of the fan (index "2") minus the total pressure upstream of the fan (index "1"):

$$\Delta p_{ts} = p_2 - p_{t,1} \tag{3}$$

To improve the energy efficiency, the shaft power (P_{shaft}) shall be as small as possible. In other words, the total-to-static efficiency defined as

$$\eta_{ts} = \frac{\dot{V} \Delta p_{ts}}{P_{shaft}} \tag{4}$$

shall be maximized. This optimization of η_{ts} is only conducted at the design flow coefficient which is $\phi_{design} = 0.14$. The corresponding design pressure coefficient is $\psi_{ts,design} = 0.15$. The design point is also indicated in Figure 1.

Some geometrical requirements exist which must be considered as constraints in the optimization. The number of blades must be exactly three (for low manufacturing costs) and the axial depth of the

rotor must not exceed $l_{ax,max} / D = 0.17$. For acoustic reasons, a strong blade sweep is desired. The selected sweep angles at hub, midspan, and tip amount to -30°, +30°, and +50°, respectively. The full description how sweep angles are geometrically implemented can be found in [1].

The design process is conducted with the software "oAX" developed at the University of Siegen. This software uses an evolutionary optimization algorithm to maximize η_{ts} with given constraints. The evaluation of the target function is conducted by artificial neural networks (ANNs) of the multi-layer perceptron (MLP) type which were trained by CFD simulations assuming a cylindrical hub and a small tip clearance ratio (S/D = 0.1%). The validity of the MLP-predicted characteristic curves is firstly confirmed by CFD simulations. Afterwards, a prototype is manufactured and examined experimentally. For series products, it is usually not affordable to realize a tip clearance of only 0.1% due to the manufacturing tolerances in terms of roundness of the housing and balancing quality of the impeller. This is considered by increasing the tip clearance to 0.5%. In addition, the cylindrical hub is often replaced by simple mounting devices, e.g. the blades are attached to a narrow disc. Figure 2 shows an example of such a design. The impact of these two geometrical changes is investigated experimentally.

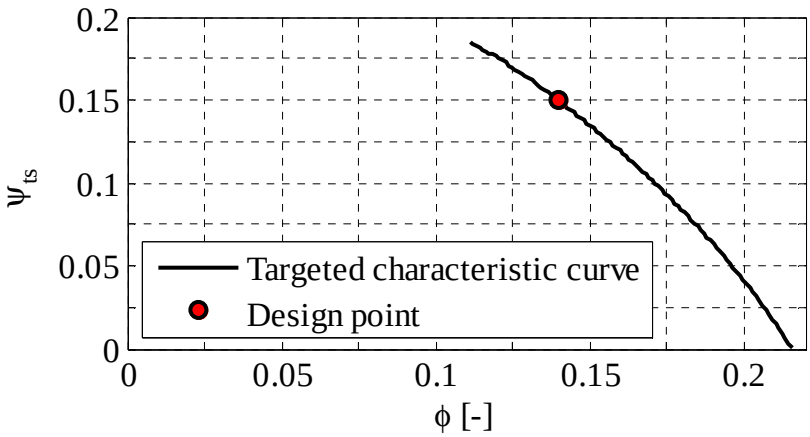

Figure 1: Targeted characteristic curves

Figure 2: Example of an industrial fan with a simple disc instead of a cylindrical hub

METHODOLOGY

Optimization strategy

The target function of the optimization is maximization of total-to-static efficiency at the design point with penalty terms for violation of the targeted pressure curve in Figure 1 and violation of geometrical constraints. Four penalty terms are considered. The first penalty term (PT_1) deals with deviations from the targeted design point:

$$PT_1 = \left| \psi_{ts,predicted} - \psi_{ts,target} \right| \text{ where } \psi_{ts,target} = 0.15 \tag{5}$$

The second penalty term is used to ensure sufficient distance from the stall point. The earliest acceptable stall point is $\phi_{stall,max}$ = 0.1. If the predicted value of ϕ_{stall} is smaller or equal, PT_2 becomes zero.

$$\begin{aligned} PT_2 &= \phi_{stall,predicted} - \phi_{stall,max} \quad \text{if} \quad \phi_{stall,predicted} - \phi_{stall,max} > 0 \\ PT_2 &= 0 \qquad\qquad\qquad\quad \text{if} \quad \phi_{stall,predicted} - \phi_{stall,max} \le 0 \end{aligned} \tag{6}$$

The third penalty term avoids a too steep decay of the pressure coefficient on the right-hand side of the design point. For that, the flow coefficient at zero total-to-static pressure rise, i.e. $\phi(\psi_{ts}=0)$, must not be earlier (i.e. at smaller values of ϕ) than the point of zero-crossing in the target curve depicted in Figure 1 where $\phi(\psi_{ts}=0)$ equals 0.22.

$$\begin{aligned} PT_3 &= \phi\left(\psi_{ts}=0\right)_{min} - \phi\left(\psi_{ts}=0\right)_{predicted} \quad \text{if} \quad \phi\left(\psi_{ts}=0\right)_{min} - \phi\left(\psi_{ts}=0\right)_{predicted} > 0 \\ PT_3 &= 0 \qquad\qquad\qquad\qquad\qquad\quad \text{if} \quad \phi\left(\psi_{ts}=0\right)_{min} - \phi\left(\psi_{ts}=0\right)_{predicted} \le 0 \end{aligned} \tag{7}$$

The last penalty term takes the axial depth into account if it exceeds the limit of $l_{ax,max}$ = 0.17 D.

$$\begin{aligned} PT_4 &= \left(l_{ax,predicited} - l_{ax,max}\right) / D \quad \text{if} \quad l_{ax,predicited} - l_{ax,max} > 0 \\ PT_4 &= 0 \qquad\qquad\qquad\qquad\quad \text{if} \quad l_{ax,predicited} - l_{ax,max} \le 0 \end{aligned} \tag{8}$$

All four penalty terms are multiplied by an empirical weighting factor (α = 5) and subtracted from the total-to-static efficiency at the design point. This yields a pseudo-efficiency η^* which is maximized by an evolutionary optimization algorithm:

$$\eta^* = \eta_{ts,predicted} - \alpha \cdot \left(PT_1 + PT_2 + PT_3 + PT_4\right) \tag{9}$$

The prediction of most of the quantities required to compute the pseudo-efficiency is done by artificial neural networks of the multi-layer perceptron (MLP) type. Only l_{ax} can directly be computed from the blade geometry and does not require an MLP. The MLPs used here are based on a previous work by the authors in 2014. The following description of the training strategy is just a summary. All details can be found in reference [1]. 26 geometrical parameters were defined and varied by a space-filling Design of Experiment (DoE). The characteristic fan performance curve of each fan design was obtained by means of Reynolds-averaged Navier-Stokes (RANS) simulations with the shear stress transport (SST) turbulence model. The computational grid consisted of approximately 500,000 hexahedral nodes and only one blade channel was simulated with periodic boundary conditions at the sides. The grid independence was proven by simulating aerodynamically optimized fans with considerably finer grids containing up to 2,000,000 nodes. It was found that the discretization error with respect to η and ψ is less than 1%. The final CFD database contains around 13,000 fan curves and was used to train the MLPs. The MLPs consist of the input layer, two hidden layers with sigmoid neurons and one output layer with linear neurons. Optimization of the hidden layer weights was done with the MATLAB Neural Network Toolbox which uses the

Levenberg-Marquandt algorithm [2]. Network structure optimization (the number of neurons in each hidden layer) was done by an in-house algorithm based on the principle ideas of the steepest descent method.

The target function evaluation by MLPs is extremely quick such that an optimization with 10,000 individuals per generation and 10,000 generations can be conducted within 30 minutes on a personal computer. The only problematic aspect about using the MLPs in the present case is that they were trained for a number of blades between five and twelve. To overcome this bottleneck, an initial optimization is conducted assuming five blades. Afterwards, two blades are eliminated and the resulting design is simulated by RANS with the CFD model described above. Of course, this design fails to meet the design pressure coefficient and the point of zero total-to-static pressure rise. Hence, the assumed value of $\psi_{ts,target}$ and $\phi(\psi_{ts}=0)$ used the corresponding penalty terms are adapted iteratively until the three-blades design meets the target curve in Figure 1.

Hub types investigated

The fan diameter for testing is the same as used for the CFD simulations, i.e. D = 300 mm. Prototype blades are milled from aluminum and can be screwed to three different hub types also milled from aluminum. The first hub type is a cylindrical body which starts 10 mm in front of the leading edge and ends 10 mm behind the trailing edge, see left picture of Figure 3. The front end of the cylinder can be a flat disc or a hemisphere. In case of the flat disc, the edge between the disc and the cylindrical surface is rounded by a radius of 5 mm. As mentioned in the introduction, manufacturing costs are often cut by using a narrow disc instead of a cylindrical hub. The corresponding hub design is shown on the right-hand side of Figure 3.

a b

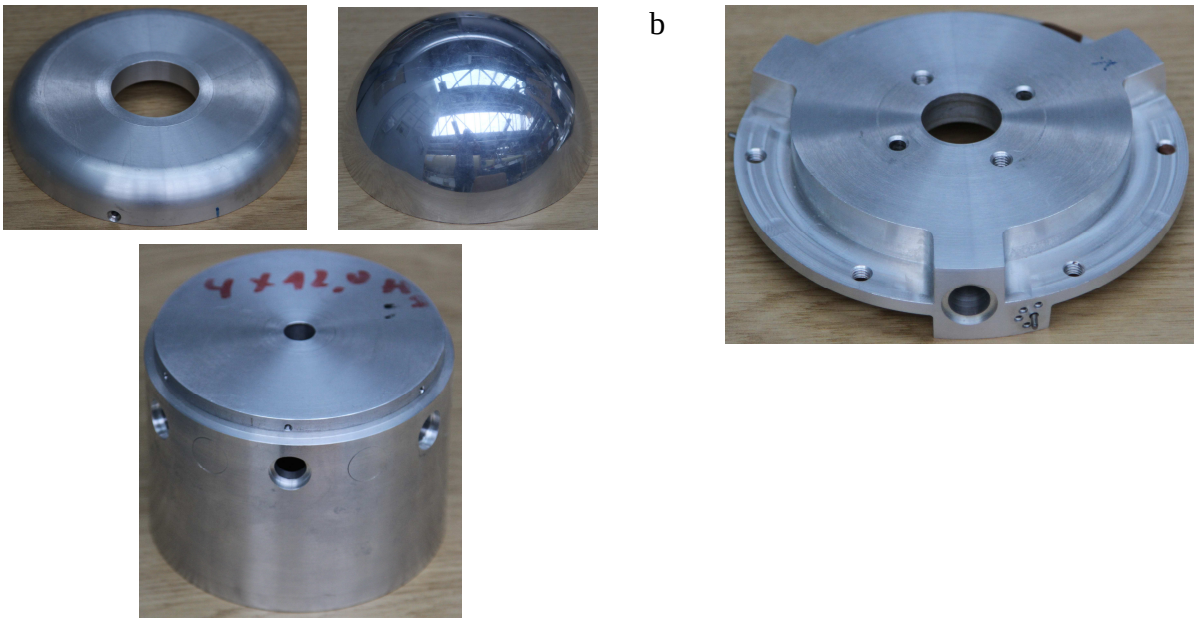

Figure 3: Hub types investigated; (a) Cylindrical hub with short (left) or hemisphical (right) spinner, (b) disc-type hub

Experimental set-up

All experimental investigations are conducted at the chamber test rig of the University of Siegen. The layout is in accordance with DIN 24163 Part 1 and Part 2 [3]. The measuring uncertainty was estimated by Hensel [4] and Winkler [5] and amounts to 1% regarding ϕ, 0.5% regarding ψ_{ts}, and 2% regarding η_{ts}. The test rig is shown in Figure 4. Air is sucked through the inlet nozzle. The pressure at the inlet nozzle is taken to compute the air velocity and consequently the flow rate. The air then passes an auxiliary fan and a throttle. These two devices are used to vary the flow rate in the interval required for the characteristic curve. Downstream of the throttle, the air is decelerated in

a large chamber. The chamber has four small holes where the pressure is taken. Due to the extremely slow velocity in the chamber, the static pressure measured is assumed to be equal to the total pressure. At the backside of the chamber, the test fan is mounted in a short duct with an inlet nozzle. The fan faces the chamber with its suction side and is driven by an electric motor. The driving power is determined by measuring the torque and the rotational speed of the shaft driving the fan.

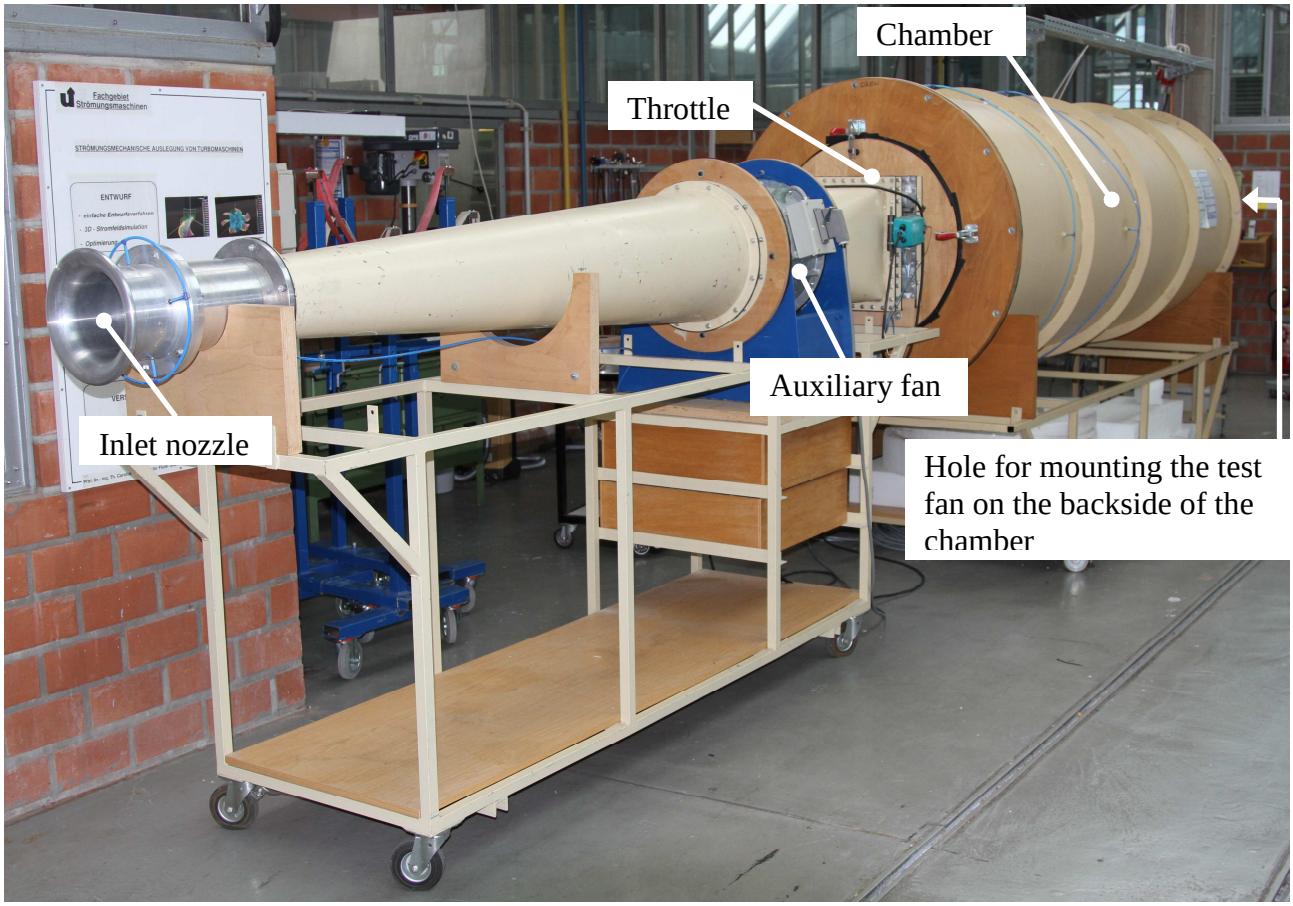

Figure 4: Chamber test rig for the measurement of characteristic fan curves at the University of Siegen

RESULTS

Optimal fan

The fan obtained from the optimization is depicted in Figure 5. Table 1 summarizes the optimal geometrical parameters. If more than one parameter is given, the values refer to equidistant locations between hub and tip and polynomials shall be used to compute values in between. Information about camber and thickness refers to modified four-digit NACA airfoils. The second column shows the values of an unconstrained optimization at the design point which are computed according to the design charts developed in [6]. The third column shows the results of the present optimization. The values differ from each other as many constraints have to be considered in the present optimization. These constraints are fulfillment of a complete characteristic curve instead of a single design point, limited axial length, given number of blades, selection of sweep angles for acoustic reasons and decrease of blade thickness from hub to tip for structural reasons. Due to these constraints, the present efficiency at the design point is around five percentage points lower as compared to a free optimization.

Validation of the CFD results

The design process included MLP-prediction and CFD-simulation of characteristic fan curves. As mentioned before, the MLP-prediction could only be conducted for five blades and is not considered in the following. Figure 6 compares the CFD-simulation with the experiment. The experimental data refers to a fan with a cylindrical hub and the same tip clearance ratio as used for CFD, i.e. S/D = 0.1%. The pressure coefficient curves show extremely good agreement. The efficiency curves differ a little stronger but still show acceptable agreement. At all operating points, the experimental result is better than CFD which makes it very unlikely that the optimization algorithm has just exploited a grid dependency or another weakness of the CFD model. Instead, it is concluded that most likely an aerodynamic optimum was found.

Table 1: optimized geometrical parameters (values in brackets refer to equidistant locations between hub and tip)

Parameter	**Optimal value according to design charts [6]**	**Value in present (constrained) optimization**	**Remark on constrained optimization**
number of blades, z	5	3	fixed
hub-to-tip ratio, ν	0.37	0.45	optimized
stagger angle, γ	[19, 30, 19, 11, 14]	[24, 22, 19, 17, 19]°	optimized
chord length ratio, c/D	[0.33, 0.24, 0.25]	[0.33, 0.33, 0.29]	optimized
max. camber ratio, f/c	[0.05, 0.05, 0.03]	[0.08, 0.08, 0.08]	optimized
pos. of max. camber ratio, x_f/c	[0.7, 0.2 ,0.55]	[0.33, 0.53, 0.7]	optimized
max. thickness ratio, d/c	[0.12, 0.05, 0.07]	[0.1, 0.08, 0.05]	fixed
pos. of max. camber ratio, x_d/c	[0.33, 0.1, 0.29]	[0.46, 0.27, 0.1]	optimized
sweep angle, λ	[+2, -5, +27]°	[-30, +30, +50]°	fixed

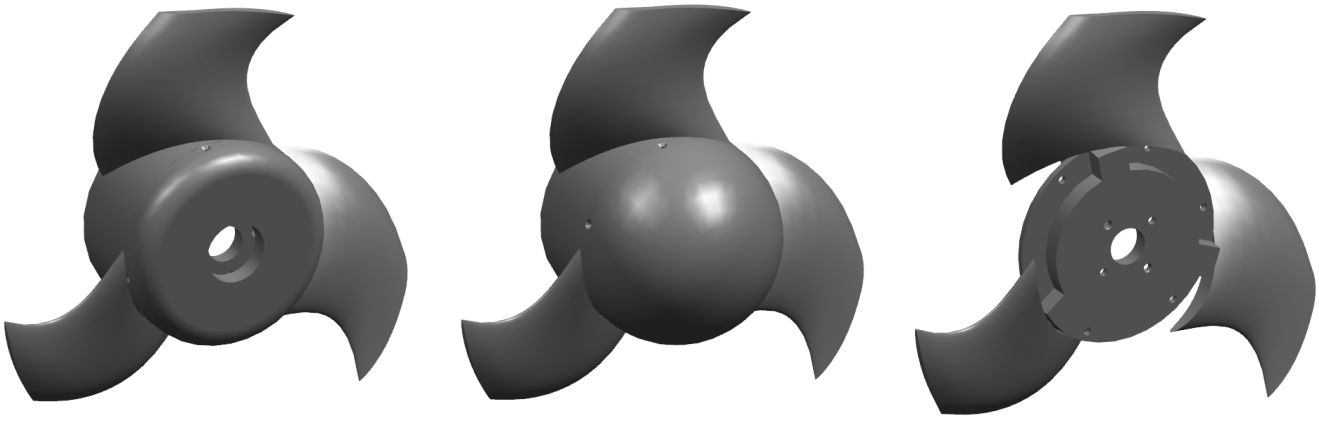

Figure 5: 3D view of the fan obtained from the optimization with distinct hub types

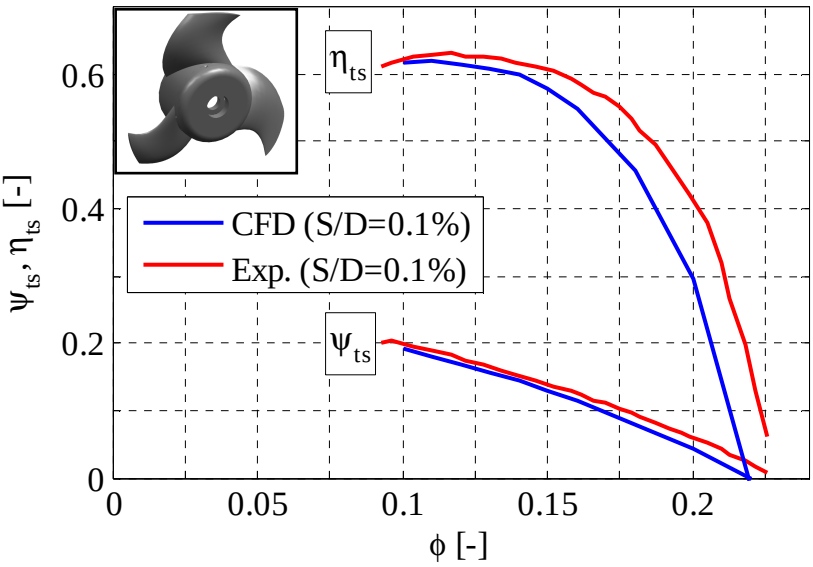

Figure 6: Comparison between CFD simulation and experiment with cylindrical hub and S/D = 0.1%

Impact of increasing the tip clearance

The tip clearance ratio is increased in two steps and additional characteristic curves are measured for S/D = 0.3% and S/D = 0.5%. The results are shown in Figure 7. The peak efficiency drops by around 3.5 percentage points for each increase of tip clearance. In addition, the operating range shrinks. The stall point moves by $\Delta\phi_{stall} \approx 0.02$ for each increase of tip clearance. From S/D = 0.1% to S/D = 0.3% there is only a minor impact on operating points with high flow coefficients. However, when increasing the tip clearance ratio to S/D = 0.5%, the performance is compromised at such operating points, too.

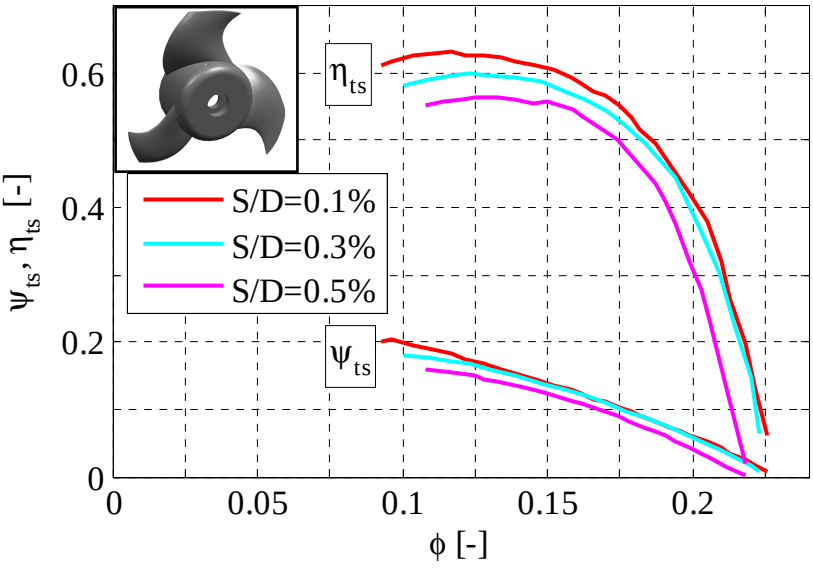

Figure 7: Measured characteristic curves of the optimized fan with cylindrical hub and varying tip clearance ratios

Impact of different hub types

For the largest tip clearance (S/D = 0.5%) the impact of the hub types is examined. The resulting characteristic curves are shown in Figure 8. Obviously, it does not make a difference weather the endplate of the cylindrical hub is equipped with a flat disc or with a hemisphere. In contrast, the

total-to-static efficiency collapses massively when using the disc hub. Thus, it seems to be most important that the blade ends on a closed surface. Using a narrow disc does not separate the blade suction from the blade pressure side and favors the generation of secondary flows. The penalty in peak efficiency amounts to more than seven percentage points. The operating range is also compromised but only on the right-hand side of the operating point. Surprisingly, the stall point is not changed and the pressure coefficient gets very close to the results obtained with the cylindrical hub in the near-stall region. However, the efficiency is reduced significantly at all operating points.

Finally, the overall impact of the geometrical modifications is illustrated by a comparison between the cylindrical hub with S/D = 0.1% and the disc hub with S/D = 0.5%, see Figure 9. A drop of peak efficiency by 14 percentage points as well as a massive reduction of operating range can be observed. The pressure coefficient shrinks by $\Delta\psi_{ts} \approx 0.03$ at most operating points and the onset of stall is shifted by $\Delta\phi \approx 0.04$.

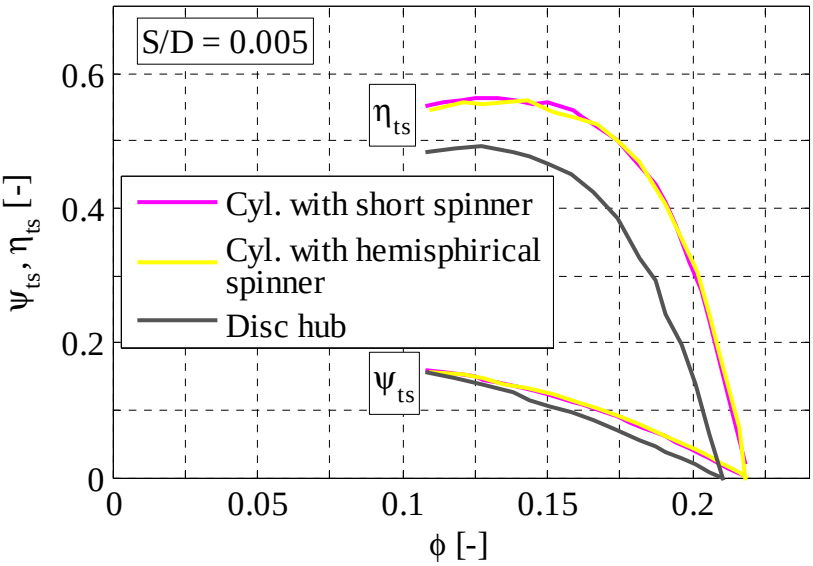

Figure 8: Measured characteristic curves for S/D = 0.5% and varying hub types

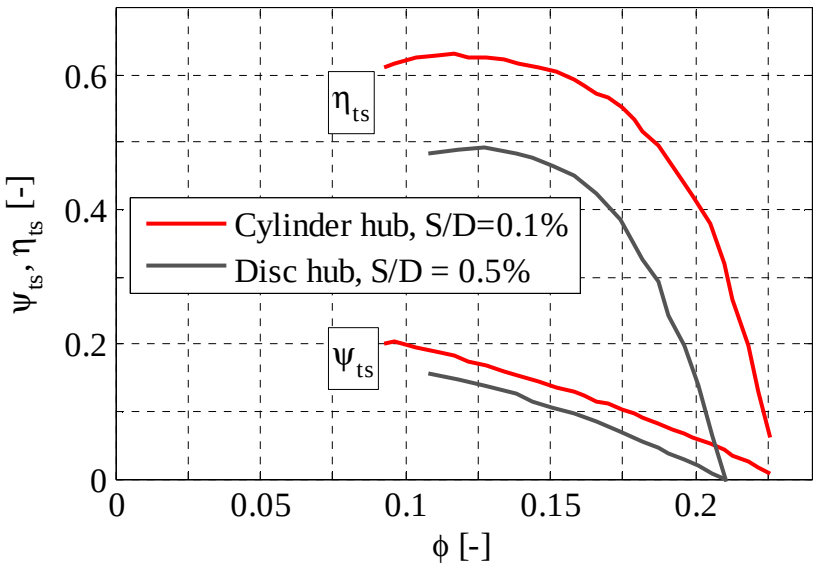

Figure 9: Measured characteristic curves of the fan directly obtained from the optimization and of a fan with both geometrical modifications (large tip clearance ratio and disc hub)

CONCLUSIONS

An axial fan was optimized for maximum total-to-static efficiency taking numerous aerodynamic and geometrical constraints into account. The optimization tool used was the software "oAX" developed at the University of Siegen. This software uses an evolutionary optimization algorithm in which the target function is evaluated by artificial neural networks. The optimization was successful since the resulting fan design fulfilled the desired characteristic curve with high efficiency. This was confirmed by both CFD-simulations and measurements. Further measurements were conducted to investigate the impact of larger (more practical) tip clearances or hubs which only consist of a narrow disc instead of a cylinder extending from leading to trailing edge. Both geometrical modifications are often applied in practice to reduce manufacturing costs of series products. However, the aerodynamic impact was found to be dramatic. The peak efficiency dropped by around seven percentage points when increasing the tip clearance from 0.1 to 0.5% of the fan diameter. In addition, the operating range was compromised, too. A further decrease of peak efficiency by more than seven percentage points was observed when replacing the cylindrical hub by a disc. Moreover, this hub type also compromised the pressure rise at operating points with large flow rates. In contrast, it is not important if the cylindrical hub has a flat front plate or a hemisphere.

It is concluded that the design methodology works quite well as long as the resulting fans are not modified afterwards. The original design always has a very small tip clearance and a cylindrical hub. The impact of modifications can be severe. If larger tip clearances and/or disc hubs are required to cut manufacturing costs, a pressure margin must be considered in the design phase. The example presented in this paper offers an estimate for the magnitude of such margins. At the present point, it is difficult to estimate to which extent the fans with the geometrical modifications still benefit from the optimization. This would require a comparison with non-optimized fans.

BIBLIOGRAPHY

[1] Bamberger, K., Carolus, T., 2014, "Performance Prediction of Axial Fans by CFD-Trained Meta-Models", *Proc. ASME TurboExpo 2014,* Düsseldorf, Germany.
[2] Marquardt, 1963, "An Algorithm for Least-Squares Estimation of Nonlinear Parameters", *SIAM Journal of Applied Mathematics*, 11, pp. 431-441.
[3] DIN 24163, 1985, "Fans; Performance Testing, Standard Characteristics," *Deutsche Norm, Berlin*.
[4] Hensel, K., 1993, "Konzeption eines Ventilatorprüfstandes nach DIN 24163 - Final thesis no. A93030003", University of Siegen, Siegen.
[5] Winkler, J., 2011, "Investigation of Trailing-Edge-Blowing on Airfoils for Turbomachinery Broad-band Noise Reduction", *PhD thesis,* University of Siegen, Siegen.
[6] Bamberger, K., Carolus, T., 2015, "Design Guidelines for Low Pressure Axial Fans Based on CFD-Trained Meta-Models", *Proc. European Turbomachinery Conference 11,* Madrid, Spain.